



## Variable responses of small and large human hepatocytes to hypoxia and hypoxia/reoxygenation (H–R)

Ricky H. Bhogal\*, Christopher J. Weston, Stuart M. Curbishley, Anand N. Bhatt, David H. Adams, Simon C. Afford

Centre for Liver Research, School of Infection and Immunity, Institute of Biomedical Research, The Medical School, The University of Birmingham, Edgbaston, Birmingham B15 2TT, UK

### ARTICLE INFO

#### Article history:

Received 15 February 2011

Accepted 21 February 2011

Available online 25 February 2011

Edited by Veli-Pekka Lehto

#### Keywords:

Human hepatocytes  
Reactive oxygen species  
Apoptosis  
Necrosis  
Hypoxia  
Liver injury

### ABSTRACT

**Hypoxia and hypoxia–reoxygenation (H–R) regulate human hepatocyte cell death by mediating the accumulation of reactive oxygen species (ROS). Hepatocytes within the liver are organised into periportal (PP) and peri-venous (PV) subpopulations. PP and PV hepatocytes differ in size and function. We investigated whether PP and PV human hepatocytes exhibit differential susceptibility to hypoxic stress. Isolated hepatocytes were used in an in vitro model of hypoxia and H–R. ROS production and cell death were assessed using flow cytometry. PV, and not PP hepatocytes, accumulate intracellular ROS in a mitochondrial dependent manner during hypoxia and H–R. This increased ROS regulates hepatocyte apoptosis and necrosis via a mitochondrial pathway. These findings have implications on the understanding of liver injury and application of potential therapeutic strategies.**

© 2011 Federation of European Biochemical Societies. Published by Elsevier B.V.

Open access under [CC BY-NC-ND license](http://creativecommons.org/licenses/by-nc-nd/3.0/).

### 1. Introduction

The functional unit of the liver is the acinus, which extends from the portal venule along the sinusoids to the terminal hepatic venule. The liver acinus in rodents extends for approximately 20 hepatocytes [1]. Peri-portal (PP) hepatocytes (zone 1) which are near the portal venule tend to be of a smaller size than peri-venous (PV) hepatocytes (zone 3) which are located near the terminal hepatic vein [2]. Indeed, some studies define and isolate PP and PV hepatocyte populations upon the basis of size [3]. Furthermore, these studies have utilised the technique of fluorescent-activated cell sorting (FACS) to consistently differentiate between PV and PP hepatocytes and study their metabolic function [4–6]. Moreover, these studies have demonstrated that these hepatocytes have distinct and separate cellular functions [3,7].

There is a large body of evidence to support the concept of morphological, biochemical and metabolic heterogeneity of small/PP and large/PV hepatocytes [7–10]. Indeed, various functions have been ascribed to specific zones of the liver acinus. Specifically, oxidative metabolism, gluconeogenesis, urea synthesis and bile formation are predominantly small/PP hepatocyte activities whereas glutamine synthesis, xenobiotic metabolism and ketogenesis are predominant functions of the large/PV hepatocytes [11,12].

Moreover, studies have shown these differences in hepatocyte function are attributable to differences in the enzyme expression [7,10].

These differences in hepatocyte function are also likely to be important determinants in the evolution of liver injury. For instance, in rodent models, it is well documented that following ischaemic liver injury, hepatocyte cell death is predominantly observed around the peri-venular region where the PV hepatocytes are located [13]. The ischaemic injury, within the liver, is regulated by the accumulation of intracellular reactive oxygen species (ROS) [14]. However, whether small/PP and large/PV hepatocytes have differential ROS accumulation during hypoxia and H–R is not known. In particular, whether small/PP or large/PV human hepatocytes exhibit differential responses to hypoxia and H–R remains to be ascertained.

Previous studies have utilised various techniques to investigate the different functions of small/PP and large/PV hepatocytes. These include retrograde digitonin perfusion of livers [8] and elutriation [7]. However, FACS analysis allows discrimination between hepatocyte subpopulations on the basis of size. Previous studies have consistently shown that the PV hepatocytes are larger in size than the PP hepatocytes [4–6]. Thus we used this latter approach to investigate whether PP or small and PV or large human hepatocytes exhibit differential responses to hypoxia and hypoxia–reoxygenation (H–R). Specifically, we investigated whether small/PP and large/PV human hepatocytes exhibit differential levels of ROS

\* Corresponding author. Fax: +44 (0) 121 415 8698.

E-mail address: [balsin@hotmail.com](mailto:balsin@hotmail.com) (R.H. Bhogal).

accumulation during hypoxia and H–R and whether this had an impact upon apoptosis and necrosis.

## 2. Materials and methods

### 2.1. Human hepatocyte isolation

Liver tissue was obtained from fully consenting patients undergoing transplantation, hepatic resection for benign liver disease or normal donor tissue surplus to surgical requirements. Liver tissue was obtained from surgical procedures carried out at the Queen Elizabeth Hospital, Birmingham, UK. Ethical approval for the study was granted by the Local Research Ethics Committee (LREC) (reference number 06/Q702/61). Human hepatocytes were isolated using a method that we have described previously [14]. Hepatocytes were isolated from fresh liver wedges weighing between 60 and 156 g using a two-step collagenase protocol. Liver wedges were first perfused with non-recirculating wash buffer (10 mM HEPES pH 7.2) (Sigma, Dorset, UK) at 37 °C using a flow rate of 75 mL/min in order to remove the remaining blood within the liver. After this, the wedge was perfused with a chelating solution (non-recirculating) (10 mM HEPES, 0.5 mM EGTA, pH 7.2) (Sigma). This was followed by further perfusion with [non-recirculating] wash buffer to remove any remaining EGTA. Following this the tissue was perfused with recirculating enzymatic dissociation solution (Hank's Balanced Salt Solution (HBSS) (Gibco, Paisley, UK) with calcium chloride (5 mM) (Sigma), magnesium chloride (5 mM) (Sigma), 0.5% w/v collagenase (Roche, Hertford, UK), 0.25% w/v protease (Sigma), 0.125% w/v hyaluronidase (Sigma) and 0.05% w/v DNase (Sigma)) at 37 °C using a flow rate 75 mL/min for between 1 and 7 min. Following manual dissociation of the liver wedge the suspension was passed through a nylon mesh of 250 µm followed by a nylon mesh of 60 µm. Suspensions were then washed at 50×g for 10 min at 4 °C in supplemented media (Dulbecco's Modified Eagle Medium (DMEM) (Gibco) with 10% v/v heat inactivated foetal calf serum (Gibco), 2 mM glutamine (Gibco), 20,000 units/L penicillin and 20 mg/L streptomycin (Gibco)). Immediately after washing cell viability was determined by trypan blue dye exclusion. Hepatocytes were plated out in supplemented media and left for 2 h. After this period, the media were changed to Williams E media (Sigma) containing hydrocortisone (2 µg/ml), insulin (0.124 U/ml), glutamine (2 mM), penicillin (20,000 units/L) and streptomycin (20 mg/L). Cells were cultured for further 2 days prior to use. Only viable cells are able to adhere to rat type 1 collagen-coated plates and hence all cells were viable at the commencement of the experiments.

Enzyme-linked immunosorbent assay (ELISA) of human hepatocytes and human hepatic sinusoidal endothelial cells (HSEC) for Cytokeratin 18, Cytokeratin 19 and CD31 were performed.

Cells (hepatocytes or HSEC) were plated on rat type 1 collagen-coated 96-well flat-bottomed plates for 24 h following isolation. Cells were then fixed in ice cold methanol for 5 min. Non-specific binding of mAb was inhibited by pre-incubation of cells for 1 h at 37 °C with 4% goat serum (Sigma) before the addition of mouse anti-human mAb (IgG Isotype-matched control (Invitrogen) CD31 (Dako), cytokeratin 19 (Dako), cytokeratin 18 (Invitrogen) for 1 h at 37 °C. The cells were then washed thoroughly before incubation with peroxidase-conjugated goat anti-mouse secondary Ab (Dako). The enzyme-linked immunosorbent assay (ELISA) was developed using *O*-phenylenediamine substrate (OPD, Dako) according to the manufacturer's instructions and the enzymatic reaction was stopped using 0.5 mol/L H<sub>2</sub>SO<sub>4</sub> (Fisher Scientific, Leicestershire, UK). Colorimetric analysis was performed by measuring absorbance values at 490 nm using a Dynatech Laboratories MRX plate reader. All treatments were performed in triplicate for each experiment.

### 2.2. Model of hypoxia and H–R injury

We utilised a model of warm in vitro hypoxia and H–R that we have described previously [14]. Briefly, in experiments, hepatocytes were cultured for 2 days at 37 °C, 5% CO<sub>2</sub> in Williams E media (Sigma) on rat type 1 collagen-coated plates. Hepatocytes were either maintained in normoxia or placed into hypoxia for 24 h, or placed into hypoxia for 24 h followed by 24 h of reoxygenation. Hypoxia was achieved by placing cells in an airtight incubator (RS Mini Galaxy A incubator, Wolf Laboratories, UK) flushed with 5% CO<sub>2</sub> and 95% N<sub>2</sub> until oxygen content in the chamber reached 0.1%, as verified by a dissolved oxygen monitor (DOH-247-KIT, Omega Engineering, UK). In preliminary experiments, human hepatocytes were exposed to 5% and 1% oxygen and no increase in ROS accumulation or cell death was noted. Therefore, we used 0.1% oxygen in all subsequent experiments for 24 h, similar to previously published studies. Additionally, Williams E media were pre-incubated in the hypoxic chamber in a sterile container, which allowed gas equilibration, for 8 h before experiments were carried out, resulting in a final oxygen concentration of <0.1% as measured with the dissolved oxygen metre. Where appropriate, after 24 h of hypoxia media were aspirated and replaced with fresh, warmed, oxygenated medium, and the cells were returned to normoxic conditions. This was defined as the beginning of reoxygenation. In experiments involving ROS inhibitors, reagents were made fresh as stock solutions and added using the correct dilutional factor to the relevant experimental wells. Specifically, 1 mM rotenone (Sigma) was dissolved in chloroform and was diluted appropriately to

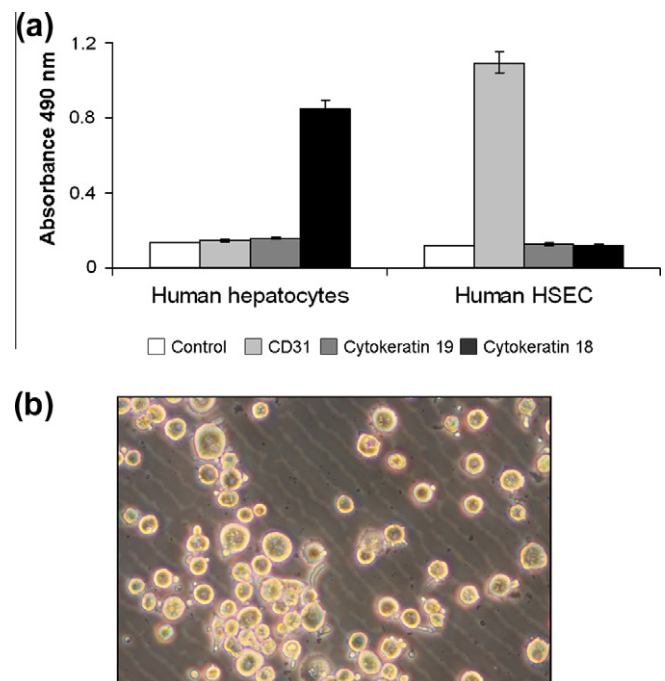


**Fig. 1.** The morphology and phenotype of isolated human hepatocytes. (a) Demonstrates the phenotypic features characteristic of human hepatocytes isolated using our protocol. The cell specific markers, cytokeratin 18, cytokeratin 19 and CD31 were determined using cell based ELISA as described in the Methods and Materials section. Human hepatocytes demonstrate a uniform staining for the hepatocyte specific marker, cytokeratin 18. These cells show no staining for the biliary epithelial marker, cytokeratin 19 or endothelial cell marker, CD31. In contrast, hepatic sinusoidal endothelial cells show strong positivity for the marker CD31 and no positivity for either cytokeratin 18 or cytokeratin 19. (b) Illustrates a representative image of human hepatocytes following successful isolation. These cells have been allowed to adhere to rat type 1 collagen for 2 h. There is a clear difference in size between the isolated hepatocytes. As previous authors have shown the smaller hepatocytes are likely to be derived from the peri-portal area and the larger hepatocytes are likely to be derived from the peri-venous region [4–6].

give working concentrations of 2  $\mu$ M. In experiments using rotenone, solvent alone controls were used to ensure no vehicle effects (data not shown). Rotenone was added at the time of placement of the cells into conditions of hypoxia or reoxygenation.

2.3. Determination of human hepatocyte ROS accumulation and apoptosis

ROS production, apoptosis and necrosis were determined by using a three-colour reporter assay system. ROS accumulation

was determined using the fluorescent probe 2',7'-dichlorofluorescein-diacetate [14]. This probe is cell permeable and once inside the cell is cleaved by intracellular esterases to 2',7'-dichlorofluorescein (DCF) (Merck, Nottingham, UK) which is then rendered cell impermeable. DCF is then able to react with intracellular ROS, specifically hydrogen peroxide, to give a fluorescent signal detectable on the FITC channel. The signal is directly proportional to the level of intracellular ROS present.

Apoptosis was determined by labelling cells with Annexin-V (Molecular Probes, Paisley, UK) which detects exposed

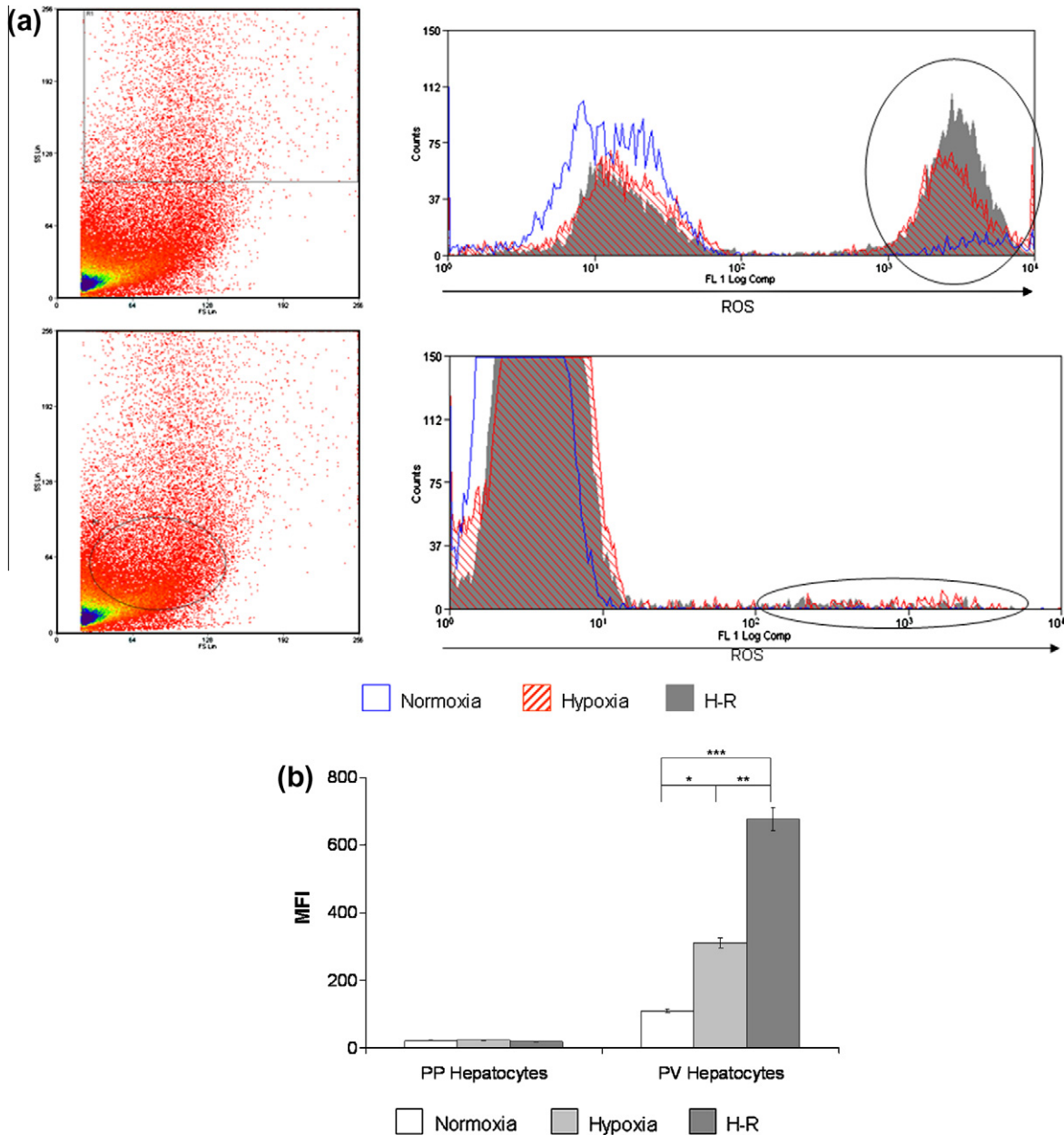


**Fig. 2.** Intracellular ROS accumulation within PP and PV human hepatocytes during hypoxia and H-R. (a) Demonstrates a representative flow cytometry plot of ROS accumulation in PP and PV primary human hepatocytes during normoxia, hypoxia and H-R. The plot on the left hand side of each flow cytometric plot represents a typical forward scatter (FS) versus side scatter (SS) plot of primary human hepatocytes. The FS versus SS plots shown is from the H-R sample of a liver preparation but similar plots were obtained during normoxia and hypoxia (data not shown). The top panel shows the gating protocol applied to human hepatocytes to analyse PV human hepatocytes. The areas of interest on the flow cytometric plots are marked by the vertical ellipses. The area on the left of each ellipse represents cell debris. Cell debris is included within the plot as human hepatocytes vary considerably in size and, therefore, to include all viable human hepatocytes in the analysis a large gate is required on the flow cytometre, this by necessity includes the cell debris. The bottom panel shows the gating protocol applied to human hepatocytes to analyse PP human hepatocytes ( $n = 5$ ). (b) Shows a bar chart with the pooled data of five separate experiments illustrating the accumulation of ROS within PV and PP human hepatocytes during hypoxia and H-R. We refer to separate experiments here as human hepatocytes isolated from separate livers (normal and diseased), used in separate experiments. Data are expressed as mean  $\pm$  S.E. (\* $P < 0.01$  relative to normoxia, \*\* $P < 0.01$  relative to hypoxia, \*\*\* $P < 0.001$  relative to normoxia, Mann-Whitney test).

phosphatidylserine on the cell membrane. 7-Amino-Actinomycin D (7-AAD) (Molecular Probes, Paisley, UK) is a vital dye that binds to DNA, only entering cells once the cell membrane is disrupted and is indicative of cellular necrosis. To ensure consistency of the flow cytometric data, each human hepatocyte preparation was labelled with DCF alone, Annexin-V alone and 7-AAD alone to ensure that cells had become labelled and that the flow cytometry data could be compensated for crossover of fluorophore emission spectra. The same flow cytometry protocol was used for all experiments shown within the study, meaning that voltages for all markers were constant for all human hepatocyte preparation ensuring internal consistency of experiments.

Following appropriate treatment of cells, media were aspirated and replaced with HBSS (Gibco) without calcium and magnesium. DCF (30  $\mu$ M) was added and the cells were incubated for 20 min in the dark at 37 °C. Next the cells were trypsinised (0.05% with EDTA, Gibco) for 5 min and washed extensively in FACS buffer (Phosphate-buffered saline pH 7.2 with 10% v/v heat inactivated foetal calf serum (Gibco). Cells were then labelled with Annexin-V and 7-AAD for 15 min whilst on ice and samples were immediately subjected to flow cytometry. At least 20,000 events were recorded within the gated region of the flow cytometer for each human hepatocyte cell preparation in each experimental condition. Only the cells within the gated region were used to calculate mean fluorescence intensity (MFI).

#### 2.4. Statistical analysis

All data are expressed as mean  $\pm$  S.E. Statistical comparisons between groups were analysed by using the Mann–Whitney test. All differences were considered statistically significant at a value of  $P < 0.05$ .

### 3. Results

#### 3.1. Isolated human hepatocytes exhibit typical features of hepatocytes

The isolated human hepatocytes consistently showed typical morphological and phenotypic features of hepatocytes (Fig. 1). The cell preparations were uniformly positive for the specific intracellular hepatocyte marker Cytokeratin 18 whilst demonstrating no staining with the biliary epithelial cell marker Cytokeratin 19 of the hepatic sinusoidal endothelial cell (HSEC) marker CD31. In contrast control HSEC demonstrates strong positivity for CD31 and no staining with Cytokeratin 18.

In addition, the isolated hepatocytes demonstrated consistent heterogeneity in terms of size. Fig. 1b clearly shows that viable intact cells were of two different size populations. As previous studies have demonstrated the small hepatocytes are highly likely to represent cells originating from the peri-portal region of the

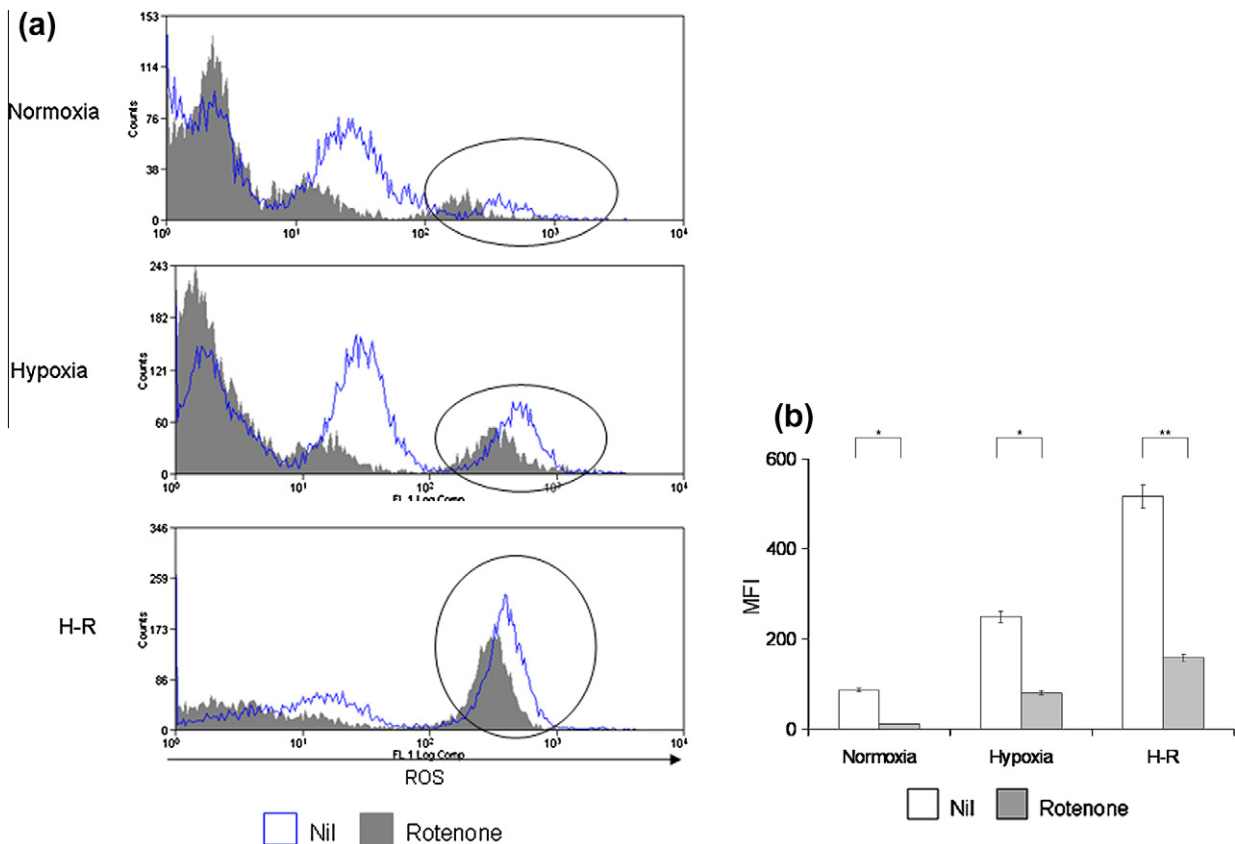


**Fig. 3.** Mitochondrial dependent ROS production in PV human hepatocytes during hypoxia and H-R. (a) Demonstrates representative flow cytometry plots to illustrate the effect of rotenone (solid grey) upon PV human hepatocyte ROS accumulation during normoxia, hypoxia and H-R. The areas of interest on the flow cytometric plots are marked by the vertical ellipses. The gating protocol applied to PV human hepatocytes is the same as that shown within Fig. 2a. Once again, the area on the left of each ellipse represents cell debris. Fig. 3b shows a bar chart with the pooled data of five separate experiments illustrating the effects of 2  $\mu$ M rotenone upon PV human hepatocytes ROS accumulation during normoxia, hypoxia and H-R. Human hepatocytes were treated with 2  $\mu$ M rotenone at the time of placement into hypoxia or H-R. Rotenone was dissolved in chloroform to make a stock solution of 1 mM and diluted appropriately. Vehicle alone was shown not to have any effect upon ROS production (data not shown). Data are expressed as MFI and readings are based upon values taken from cells within the gated region shown in Fig. 2a. Data are expressed as mean  $\pm$  S.E. (\* $P < 0.01$  relative to basal, \*\* $P < 0.001$  relative to basal).

liver whereas the larger hepatocytes represent those from the peri-venular region [4–6]. These data demonstrate that our isolation technique yielded human hepatocytes of a high purity with little or no contamination with other cell types and that using FACS we could discriminate effectively between small/PP and large/PV human hepatocytes.

### 3.2. Small (PP) and large (PV) human hepatocytes exhibit differential ROS accumulation during hypoxia and H–R

FACS analysis was able to discriminate between large or PV and small or PP human hepatocytes using appropriate forward scatter (FS) and side scatter (SS) plots (Fig. 2). Accordingly, using suitable flow cytometric gating protocols the response of large/PV and small/PP hepatocytes to hypoxia and H–R could be ascertained.

PV hepatocytes, isolated from benign liver resections, normal donor tissue and biliary cirrhosis (primary biliary cirrhosis and primary sclerosing cholangitis) showed significant increase in ROS accumulation during hypoxia (Fig. 2a and b). Exposure of human hepatocytes to H–R further accentuated intracellular ROS accumulation. In contrast, PP hepatocytes, showed no increase in intracellular ROS accumulation during hypoxia and H–R.

### 3.3. ROS production in large (PV) hepatocytes is mitochondrial dependent

Numerous previous studies have shown that the mitochondrion is the central source of ROS during hypoxia and H–R [14–16]. Therefore, mitochondrial function was inhibited within large/PV human hepatocytes using the complex I mitochondrial chain inhibitor, rotenone. As Fig. 3a and b demonstrates, rotenone

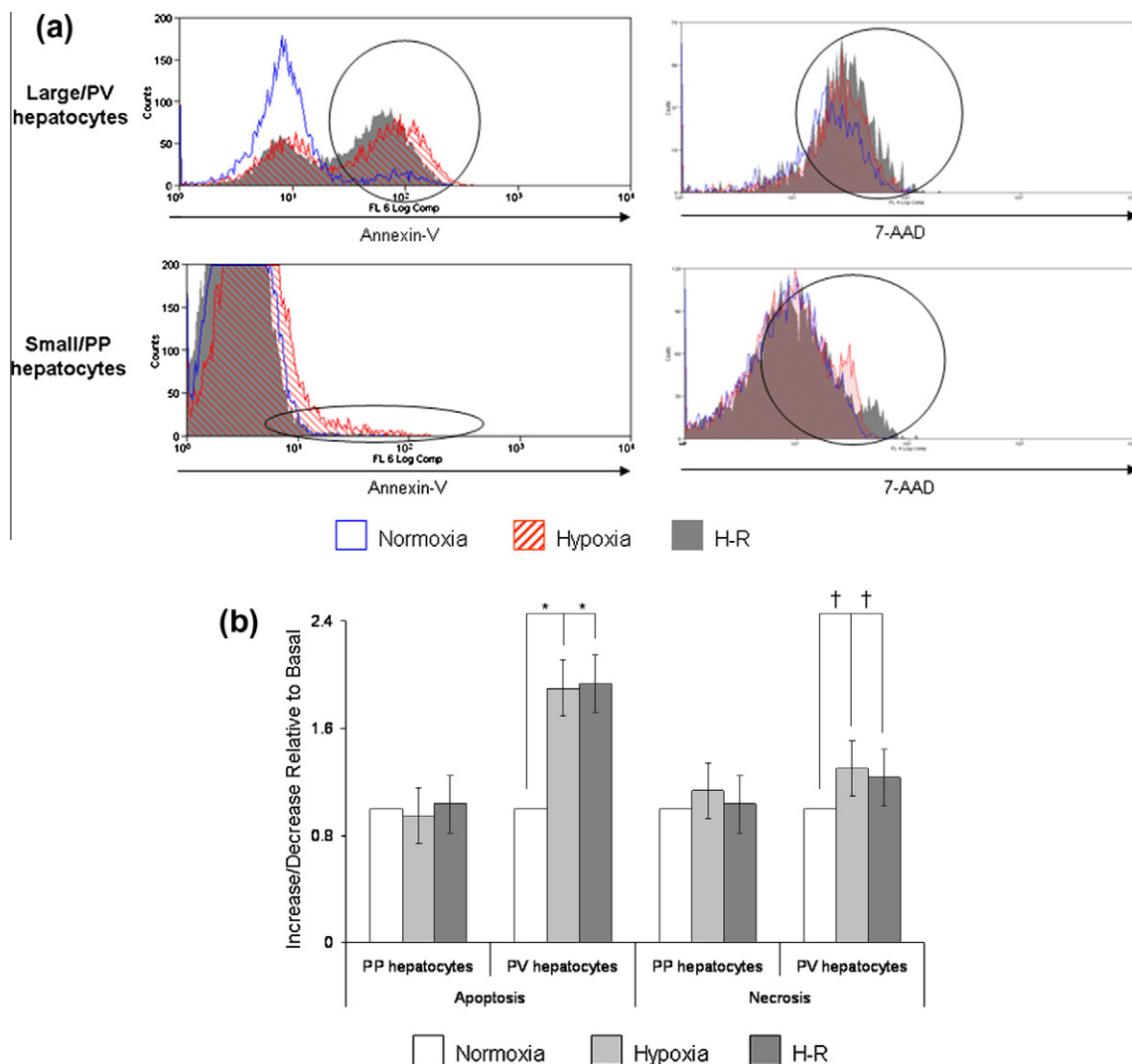


**Fig. 4.** PV human hepatocytes undergo apoptosis and necrosis during hypoxia and H–R. (a) Shows representative flow cytometry plots to illustrate the level of apoptosis and necrosis in PP and PV human hepatocytes during hypoxia and H–R. The gate used to analyse primary human hepatocytes are the same as that shown in Fig. 2. The area of interest within the flow cytometric plots are marked by the vertical ellipses. (b) Shows a bar chart with the pooled data of five separate experiments illustrating the level of apoptosis and necrosis in PP and PV human hepatocytes during hypoxia and H–R. Data are expressed as increase/decrease relative to basal, where basal refers to the level of apoptosis and necrosis during normoxia alone. Data are expressed as mean  $\pm$  S.E. ( $^{\dagger}P < 0.05$  relative to basal,  $^*P < 0.01$  relative to basal). (c) Shows representative flow cytometry plots to illustrate the effects of rotenone upon the level of PV human hepatocyte apoptosis and necrosis during normoxia, hypoxia and H–R. The gating protocol used to analyse large human hepatocytes is the same as that shown in Fig. 2. The area of interest within the flow cytometric plots are marked by the vertical ellipses. (d) Shows a bar chart with the pooled data of five separate experiments illustrating the effect of rotenone upon the level of PV hepatocyte apoptosis and necrosis during normoxia, hypoxia and H–R. Data are expressed as increase/decrease relative to basal, where basal refers to the level of apoptosis and necrosis during normoxia alone. Data are expressed as mean  $\pm$  S.E. ( $^{\dagger}P < 0.05$  relative to no treatment in the same experimental condition,  $^*P < 0.01$  relative to no treatment in the same experimental condition,  $^{**}P < 0.001$  relative to no treatment in the same experimental condition).

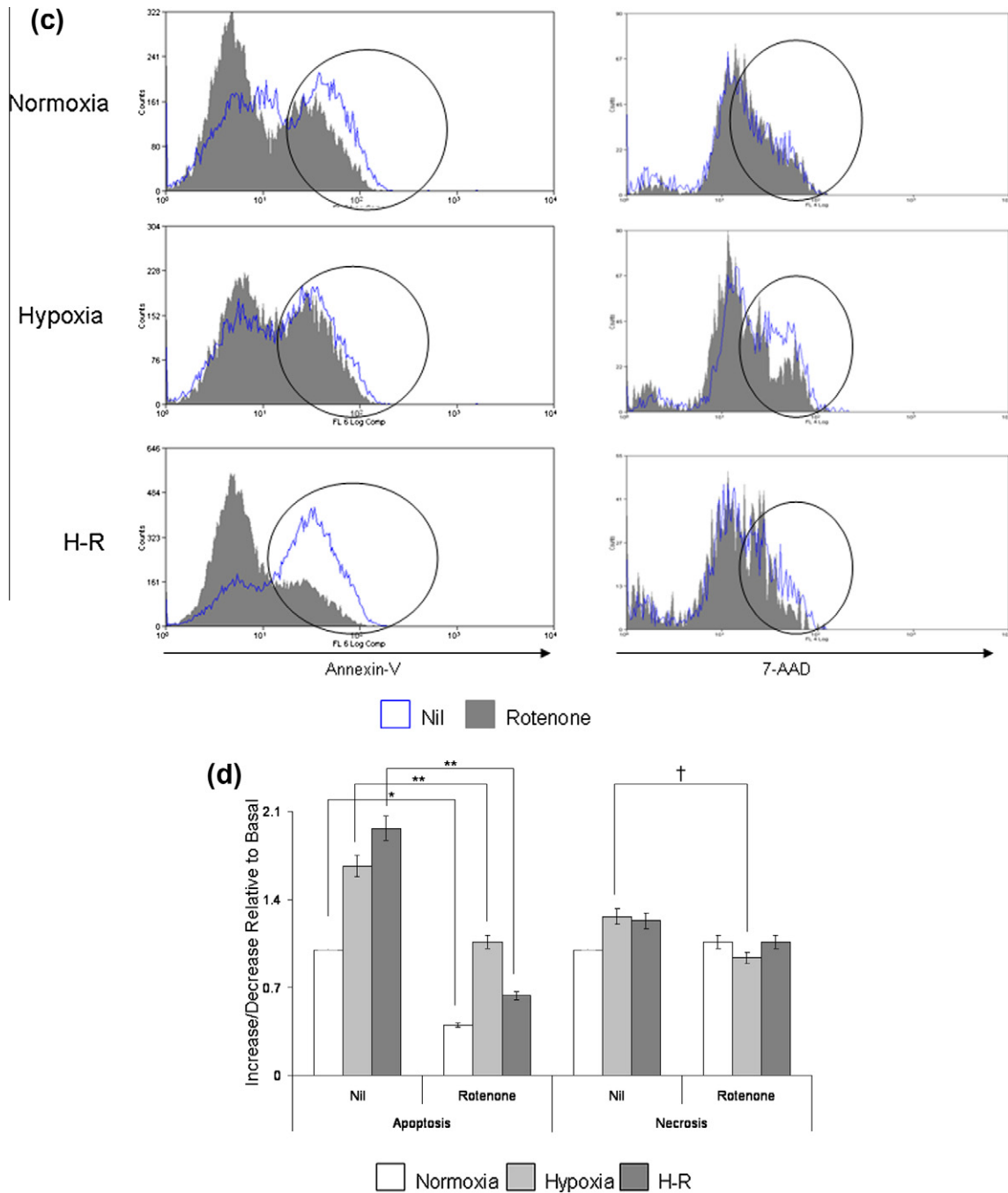


Fig. 4 (continued)

significantly reduced ROS accumulation in large/PV human hepatocytes during normoxia, hypoxia and H-R. Rotenone had no effect upon ROS accumulation in small/PP human hepatocytes (data not shown).

#### 3.4. Large (PV) and not small (PP) human hepatocytes undergo apoptosis and necrosis during hypoxia and H-R

The relationship between intracellular ROS accumulation and apoptosis and necrosis has been clearly established within human hepatocytes [14]. Accordingly, we found that large/PV human hepatocytes, in line with their propensity to generate ROS during hypoxia and H-R, underwent significant levels of apoptosis and necrosis (Fig. 4a and b). In contrast, small/PP hepatocytes did not

undergo any apoptosis or necrosis in line with their lack of ROS generation during hypoxia and H-R. We finally investigated whether mitochondrial generated ROS during hypoxia and H-R was responsible for regulating human hepatocyte apoptosis and necrosis. As Fig. 4c and d illustrates, rotenone significantly reduces large/PV human hepatocyte apoptosis and necrosis during normoxia, hypoxia and H-R. These findings clearly demonstrate that in PV human hepatocytes mitochondrial ROS generated during hypoxia and H-R drives cell death.

#### 4. Discussion

Exposure of hepatocytes to pathological conditions in a micro-environment of hypoxia and H-R is very frequent in several hepa-

tic diseases and hepatic surgery. These include haemodynamic shock, septicaemia and liver transplantation. Death of hepatocytes by hypoxia and H–R injury is a multifactorial event including alteration of the plasma membrane, increase of autophagic vacuoles, rupture of blebs on the cell surface, calcium accumulation and mitochondrial damage [9]. The common mediator of these death pathways appears to be the accumulation of ROS [17]. Studies in rodent models suggest that large/PV hepatocytes are more vulnerable to damage during hepatic injury [8]. Moreover, hepatocyte proliferation, which is an important determinant of patient survival after major hepatic resection, occurs from the small/PP to large/PV hepatocytes. Therefore, an understanding of the differential vulnerability of hepatocytes to liver injury would provide an important basis for preventing loss of liver function and/or failure caused by cirrhosis, hepatic resection and liver transplantation [8]. Common factors to most liver injuries are hypoxia and the generation of ROS [14,17]. However, the susceptibility of hepatocytes, and in particular human hepatocytes, to oxidative stress has not been assessed directly. We show for the first time to our knowledge, clear evidence that large/PV hepatocytes are the most susceptible to hypoxic injury. Moreover, this susceptibility is due to the greater propensity of the mitochondria of these large/PV hepatocytes to produce and accumulate intracellular ROS [18]. It must be noted however, that inhibiting mitochondrial function does not completely abrogate large/PV human hepatocyte apoptosis and necrosis. Indeed, previous studies have shown that other enzymes involved in ROS generation are also involved in regulating human hepatocyte apoptosis [14].

The increased level of apoptosis and necrosis seen in large/PV human hepatocytes seen *in vitro* in the present study would concur with *in vivo* models of murine and rodent liver injury, where cell death is observed in the peri-venular regions of the liver [13]. A possible explanation for this observation may well be that the powerful antioxidant glutathione (in rodent models) varies considerably in concentration between hepatocytes isolated from the small/PP and large/PV regions [19]. Specifically, large/PV hepatocytes have less intracellular glutathione when compared to small/PP or small hepatocytes. Moreover, following stimulation with amino acids larger hepatocytes are able to generate less intracellular glutathione than small hepatocytes [19]. These findings could in theory explain the increased susceptibility of large/PV human hepatocytes to hypoxic injury.

Previous studies have shown that mitochondrial inhibitors and anti-oxidants inhibit ROS accumulation in human hepatocytes during hypoxia and H–R [14–16]. Our present study builds upon this observation, demonstrating that mitochondrial electron transport chain inhibitors specifically reduce ROS accumulation in the large/PV hepatocytes and consequently reduce apoptosis in this population during hypoxia and H–R. Many studies have suggested that resident liver macrophages (Kupffer cells) located in the PV region of liver are activated during ischaemia and release ROS, leading to hepatocyte damage [8]. Taken together with our study this suggests that the PV region of the liver is the preferential site of hepatic inflammation and ROS generation during hypoxic liver injury. Contrastingly, some studies in rodent hepatocytes have suggested that small/PP hepatocytes are more vulnerable to hypoxic injury due to their higher requirement of oxygen [8]. We remain uncertain about the explanation for these discrepancies which may represent inter-species differences of unknown aetiology.

In conclusion, large/PV human hepatocytes are the most susceptible to hypoxic damage. This suggests that therapeutics used

in the treatment of liver disease may primarily act upon PV or large human hepatocytes. In the future, therapeutic strategies used to treat hepatic inflammation may require novel drug targeting methods that allow the delivery of the drug preferentially to the PV or large hepatocytes.

## Acknowledgements

R.H.B. is in receipt of a Wellcome Trust Fellowship (DDDP.RCHX14183). The authors would like to thank the clinical team at the Queen Elizabeth Hospital, Birmingham for the procurement of liver tissue.

## References

- [1] Loud, A.V. (1968) A quantitative stereological description of the ultrastructure of normal rat liver parenchymal cells. *J. Cell Biol.* 37, 27–46.
- [2] Schmuker, D.L., Mooney, J.S. and Jones, A.L. (1978) Stereological analysis of hepatic fine structure in the Fischer 344 rat. Influence of sublobular location and animal age. *J. Cell Biol.* 78, 319–337.
- [3] Willson, R.A., Wormsley, S.B. and Muller-Eberhard (1984) A comparison of hepatocyte size distribution in untreated and Phenobarbital-treated rats as assessed by flow cytometry. *Dig. Dis. Sci.* 29, 753–757.
- [4] Braakman, I., Keij, J., Hardonk, M.J., Meijer, D.K.F. and Groothuis, G.M. (1991) Separation of periportal and perivenous rat hepatocytes by fluorescence-activated cell sorting: confirmation with colloidal gold and exogenous marker. *Hepatology* 13, 73–82.
- [5] Thalhammer, T., Gessl, A., Braakman, I. and Graf, J. (1989) Separation of hepatocytes of different acinar zones by flow cytometry. *Cytometry* 10, 772–778.
- [6] Gumucio, J.J., May, M., Dvorak, C., Chianale, J. and Massey, V. (1986) The isolation of functionally heterogeneous hepatocytes of the proximal and distal half of the liver acinus in the rat. *Hepatology* 6, 932–944.
- [7] Wilton, J.C., Chipman, K., Lawson, C.J., Strain, A.J. and Coleman, R. (1993) Periportal- and perivenous-enriched hepatocyte couplets: differences in canalicular activity and in response to oxidative stress. *Biochem. J.* 292, 773–779.
- [8] Taniai, H., Hines, I.N., Bharwani, S., Maloney, R.E., Nimura, Y., Gao, B., et al. (2004) Susceptibility of murine periportal hepatocytes to hypoxia-reoxygenation: role for NO and Kupffer cell-derived oxidants. *Hepatology* 39, 1544–1552.
- [9] Massip-Salcedo, M., Rosello-Catafau, J., Prieto, J., Avila, M.A. and Peralta, C. (2007) The response of the hepatocyte to ischemia. *Liver Int.* 27, 6–17.
- [10] Bella, D.L., Hirschberger, L.L., Kwon, Y.H. and Stipanuk, M.H. (2002) Cysteine metabolism in periportal and perivenous hepatocytes: perivenous cells have greater capacity for glutathione production and taurine synthesis but not for cysteine catabolism. *Amino Acids* 23, 453–458.
- [11] Jungerman, K. and Katz, N. (1989) Functional specialization of different hepatocyte populations. *Physiol. Rev.* 69, 708–763.
- [12] Traber, P., Chianale, J. and Gumucio, J.J. (1988) Physiologic significance and regulation of hepatocellular heterogeneity. *Gastroenterology* 95, 1130–1143.
- [13] Kato, Y., Tanaka, J. and Koyama, K. (2001) Intralobular heterogeneity of oxidative stress and cell death in ischemia-reperfused rat liver. *J. Surg. Res.* 95, 99–106.
- [14] Bhogal, R.H., Curbishley, S.M., Weston, C.J., Adams, D.H. and Afford, S.C. (2010) Reactive oxygen species mediate human hepatocyte injury during hypoxia/reoxygenation. *Liver Transpl.* 16, 1303–1313.
- [15] Lluís, J.M., Buricchi, F., Chiarugi, P., Morales, A. and Fernandez-Checa, J.C. (2007) Dual role of mitochondrial reactive oxygen species in hypoxia signalling: activation of nuclear factor- $\kappa$ B via c-SRC- and oxidant dependent cell death. *Cancer Res.* 67, 7368–7377.
- [16] Lluís, J.M., Morales, A., Blasco, C., Colell, A., Mari, M., Garcia-Ruiz, C., et al. (2005) Critical role of mitochondrial glutathione in the survival of hepatocytes during hypoxia. *J. Biol. Chem.* 280, 3224–3232.
- [17] Andrade Jr, D.R., Andrade, D.R. and Santos, S.A. (2009) Study of rat hepatocytes in primary culture submitted to hypoxia and reoxygenation: action of the cytoprotectors prostaglandin E1, superoxide dismutase, allopurinol and verapamil. *Arq. Gastroenterol.* 46, 333–340.
- [18] Baraona, E., Jauhonen, P., Miyakawa, H. and Lieber, C.S. (1983) Zonal redox changes as a cause of selective perivenular hepatotoxicity of alcohol. *Pharmacol. Biochem. Behav.* 18, 449–454.
- [19] Kera, Y., Penttilä, K.E. and Lindros, K.O. (1988) Glutathione replenishment capacity is lower in isolated perivenous than in periportal hepatocytes. *Biochem. J.* 254, 411–417.